

Molecular docking studies on arbutin analogues as inhibitors of tyrosinase enzyme

Études d'amarrage moléculaire sur les analogues d'arbutine en tant qu'inhibiteurs de l'enzyme tyrosinase

Sabrina Benouis^{1*}, Fouad Ferkous¹, Khairedine Kraim², Ahmed Allali³ & Youcef Saihi¹

¹Laboratoire de chimie organique appliquée, Faculté des Sciences, Université Badji Mokhtar, BP12, 23000, Annaba, Algérie.

²Ecole normale supérieure d'enseignement technologique de Skikda(ENSET), 21000, Azzaba, Skikda, Algérie.

³Département des Sciences Biologiques, Université d'El Oued, BP 789, 39000, El Oued-Algérie.

Article Info

Article history:

Received 13/03/2019

Revised 08/05/2019

Accepted 22/05/2019

Keywords

Arbutin, Molecular docking,
Tyrosinase, Inhibition.

Mots clés

Arbutine, Amarrage
Moléculaire, Tyrosinase,
Inhibition

ABSTRACT

The arbutin presents the starting point of our work which aims to discover new inhibitors of the tyrosinase enzyme. Therefore, we have studied the activity of arbutin derivatives as inhibitors against mushroom tyrosinase based on the molecular docking.

Molecular docking studies were performed on a series of arbutin analogues retrieved from Zinc database (with 70% as similarity threshold). The arbutin analogues were docked within the active site region of mushroom tyrosinase (PDB: 2Y9X) using Molegro Virtual Docker V.5.0.

The results of molecular docking studies revealed that some analogues of arbutin have higher Moldock score (in terms of negative energy) than arbutin and the experimentally known inhibitors of tyrosinase, and showed favourable molecular interactions exhibiting common molecular interaction with Met280, His85, His61 and Asn260 residues of tyrosinase. Furthermore, the top docked compounds used in this work do not violate the Lipinsky rule of five.

RESUME

L'arbutine constitue le point de départ de notre travail visant à découvrir de nouveaux inhibiteurs de l'enzyme tyrosinase. Par conséquent, nous avons étudié l'activité des dérivés de l'arbutine en tant qu'inhibiteurs de la tyrosinase de champignon, basée sur l'amarrage moléculaire.

Des études d'amarrage moléculaire ont été effectuées sur une série d'analogues d'arbutine extraites de la base de données Zinc (avec un taux de similarité de 70%). Les analogues d'arbutine ont été amarrés dans la région du site actif de la tyrosinase de champignon (PDB: 2Y9X) à l'aide du logiciel Molegro Virtual Docker V.5.0.

Les résultats des études d'amarrage moléculaire ont révélé que certains analogues de l'arbutine présentent un score Moldock (en termes d'énergie négative) plus élevé que celui de l'arbutine et des inhibiteurs de la tyrosinase expérimentalement connus, et qu'ils montrent des interactions moléculaires favorables présentant une interaction moléculaire commune avec les résidus de la tyrosinase : Met280, His85, His61 et Asn260. En outre, les principaux composés amarrés utilisés dans ce travail respectent la règle des cinq de Lipinsky.

*Corresponding Author

Sabrina Benouis

Laboratoire de chimie organique appliquée, Faculté des Sciences, Université Badji Mokhtar,
BP 12, Annaba, 23000, Algérie.

Email: s.benouis@gmail.com

1. INTRODUCTION

Since antiquity, nature has been a source of the majority of medicines, cosmetics and bioactive compounds [1-4]. Until now, plants play a vital role in the pharmacological, agricultural and food industry [5-7]. Arbutin is one of the natural bioactive compounds extracted from plants, recognized for its medicinal properties and its pharmacological activities such as: gastroprotective [8], antimicrobial [9], antitumor [10], antioxidant [11] and anti-inflammatory [12] activities. Moreover, arbutin is widely used in cosmetics as a depigment agent for its effective effect on hyperpigmentation of the skin [13-15]. Tyrosinase is the enzyme responsible for the production of melanin [16], natural substance responsible for the pigmentation of the skin [17]. The Arbutin presents the starting point of our work which aims to discover new inhibitors of the enzyme tyrosinase. In this study, we have realized a virtual screening based on molecular docking of 1584 analogues of arbutin as inhibitors against the mushroom tyrosinase. The aim of this work is to identify the binding mode of the active molecules and to predict the affinity of ligand and protein using Moldock scoring function installed in the MVD program [18].

2. RESEARCH METHODS

2.1. TARGET ENZYME

The Tyrosinase, extracted from *Agaricus Bisporus* mushroom, was selected as the target enzyme. The three-dimensional structure of the target enzyme was taken from the Protein Data Bank (PDB ID: 2Y9X) [19]. The selected target (ID: 2Y9X) represents the L4H4 octamer (four L-H dimer) crystal structures of tyrosinase from *Agaricus Bisporus* mushroom [20] with a resolution of 2.78 Å. The tyrosinase domain represented by the H1 subunit and containing the binuclear copper binding site is selected to perform the molecular docking studies [21]. The active site complexed with the reference inhibitor tropolone is conserved with the binuclear copper atoms. The water molecules are removed from the binding site and the enzyme was prepared with Molegro Virtual Docker by adding hydrogen atoms, and all atoms types and bond orders were corrected.

2.2. LIGANDS DATASET: CHEMICAL SIMILARITY SEARCHING

The three-dimensional structure of arbutin (Zinc04104676) and his analogues were retrieved from the public free Zinc database [22]. We have adopted the tanimoto coefficient as search parameters with 70% as similarity threshold. All obtained structures are saved as "mol2" files for our docking studies. The library is prepared then with MVD program.

2.3. MOLECULAR DOCKING

When the three-dimensional structure is known, the binding affinity between ligand and enzyme is treated with molecular docking. Here the molecular docking studies were performed with the program Molegro Virtual Docker. The program is based on three principal algorithms: Moldock scoring function, conformational search algorithm and cavity prediction algorithm, represented as follow:

a. MOLDOCK SCORING FUNCTION

Proposed by Gelhaar et al [23] and is composed of two terms representing respectively the intramolecular energy (the interaction between atoms of the same ligand) and external interaction energy (ligand – protein). The pose energy (enzyme –ligand) is represented by the sum of these two energy terms and their expressions are defined as follow:

$$E_{score} = E_{inter} + E_{intra}$$

Where:

E_{inter} and E_{intra} are the ligand–protein energy interaction and the ligand internal energy respectively.

$$E_{inter} = \sum_{i \in \text{ligand}} \sum_{j \in \text{protein}} \left[E_{PLP}(r_{ij}) + 332.0 \frac{q_i q_j}{4r_{ij}^2} \right]$$

Where:

- E_{PLP} : is piecewise linear potential function;
- q_i and q_j : are the electrical charges of the atoms i and j ;

- r_{ij} : is the distance between the two atoms i and j (i is ligand atom, and j is protein atom).

$$E_{intra} = \sum_{i \in \text{ligand}} \sum_{j \in \text{ligand}} E_{PLP}(r_{ij}) + \sum_{\text{flexiblebonds}} [1 - \cos(m \cdot \theta - \theta_0)] + E_{clash}$$

Where:

- The first term calculates all the energies involving pairs of atoms of the ligand, except those connected by two bonds;
- The last two terms represent respectively the torsional energy and a penalty of 1000 kcal/mol if the distance between two heavy atoms is less than 2.0Å.

b. MOLDOCK OPTIMIZER

Moldock Optimizer, used as a search algorithm by the MVD program, is an iterative optimization technique inspired from the evolution theory of Darwin. The Moldock algorithm randomly generates the first population. Then, the poor solutions are weeded out and the good candidate solutions are selected and modified using crossover and mutation operations between the candidate solutions (poses) [24].

c. CAVITY PREDICTION

The grid-based prediction algorithm is used in order to determine the binding site. This algorithm divides the protein space into a discrete grid with a resolution of 0.8Å and at each point of the grid is placed a sphere of radius 1.4Å. The detected cavities are ranked according to their volume. The binding site was detected, selected as space search and centred on the co-crystallized troplone with a radius of 14Å. During the docking simulation, the program generates several poses for each ligand using the Moldock scoring function and Moldock optimizer algorithms. The parameters of the last algorithm are; the population size, maximum iterations, scaling factor, and crossover rate were set to 100; 9000; 0.50 and 0.90 respectively. For each complex, the molecular docking simulation was executed 100 runs while each run returns one pose. The resulting poses were visualized in table 1.

Table 1. Docking score for the top ten ranked hits with known experimentally tyrosinase inhibitors.

Compound ID	E-Inter (cof - lig) ^a (kcal.mol ⁻¹)	E-Inter (pro - lig) ^b (kcal.mol ⁻¹)	E-Inter total ^c (kcal.mol ⁻¹)	MolDock score (kcal.mol ⁻¹)	H-bond energy ^d (kcal.mol ⁻¹)
Zinc03978768	-3.451	-155.717	-159.168	-138.301	-8.659
Zinc31160316	-5.056	-149.988	-155.044	-127.429	-5.000
Zinc28002398	-3.984	-142.775	-146.758	-125.788	-4.923
Zinc28005633	1.193	-147.886	-146.693	-123.878	-9.988
Zinc13542698	0.723	-134.729	-134.007	-114.494	-11.609
Zinc38213972	-4.865	-125.419	-130.284	-114.467	-8.652
Zinc05665673	0.000	-133.558	-148.413	-114.272	-14.855
Zinc67902575	-4.684	-131.776	-136.460	-113.987	-10.00
Zinc04201163	-2.389	-130.830	-133.219	-109.393	-9.147
Zinc03149174	-1.369	-123.643	-131.544	-107.582	-7.901
Arbutin	-2.411	-111.299	-113.709	-89.877	-12.752
Kojic acid	-5.043	-78.238	-83.282	-70.911	-6.219
Tropolone	0.269	-70.428	-70.159	-61.024	-2.104

^a: The total ligand-cofactor interaction energy.

^b: The total pose-protein interaction energy.

^c: The total interaction energy.

^d: Hydrogen bonding energy.

3. RESULTS AND ANALYSIS

The protein structure complex of the inhibitor of reference with tyrosinase enzyme (PDB ID: 2Y9X) was obtained from the Protein database. The potential ligand binding cavity was predicted using Molegro Virtual Docker for the mushroom tyrosinase which has a volume of 50.69Å³ and a surface area of 197.12Å² (Fig. 1).

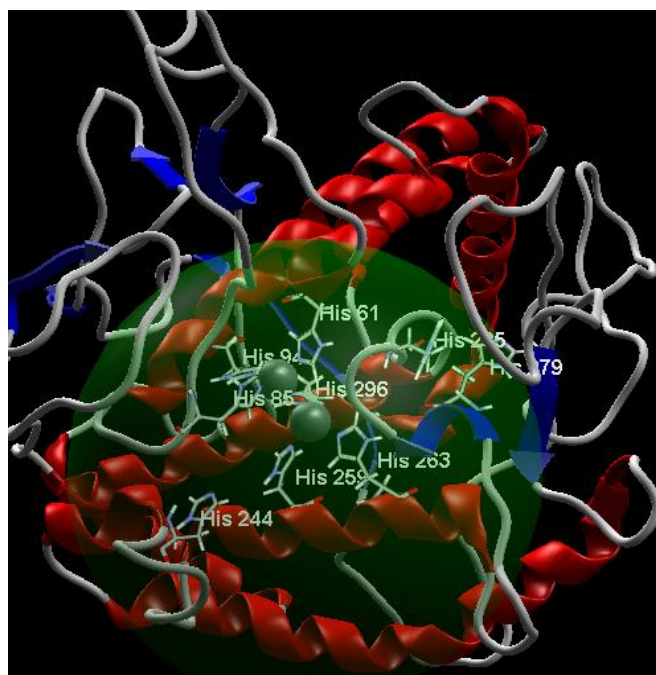


Figure 1. The binding cavity of tyrosinase enzyme with residues Phe264, Phe90, His94, His244, Phe292, Ala286, Val283, Gly281, Met280, Asn260, Ser289, His85, His61, His263, His259 and copper ions represented by two silver balls.

Molecular docking was carried out and the top poses docked at the active site region of tyrosinase were ranked according to the MolDock score energy (Table 1). From the docking result obtained, we notice that the arbutin analogues (Zinc03978768, Zinc31160316, Zinc28002398, Zinc28005633, Zinc13542698, Zinc38213972, Zinc05665673, Zinc67902575, Zinc04201163, Zinc03149174) have higher MolDock scores (in term of negative energy) than arbutin and the experimentally known tyrosinase inhibitors.

The top ranked arbutin analogues present a high level of ligand-protein interaction energy compared to arbutin and experimentally tyrosinase inhibitors like Kojic acid [25] and tropolone [26]. The correlation between the hydrogen bonding energy and molecular weight for the top ranked compounds is calculated and depicted in Figure 2. A low value of determination coefficient (0.09) was obtained, which indicates that the predicted hydrogen bonding energy was due to the structure features and not because of its molecular size.

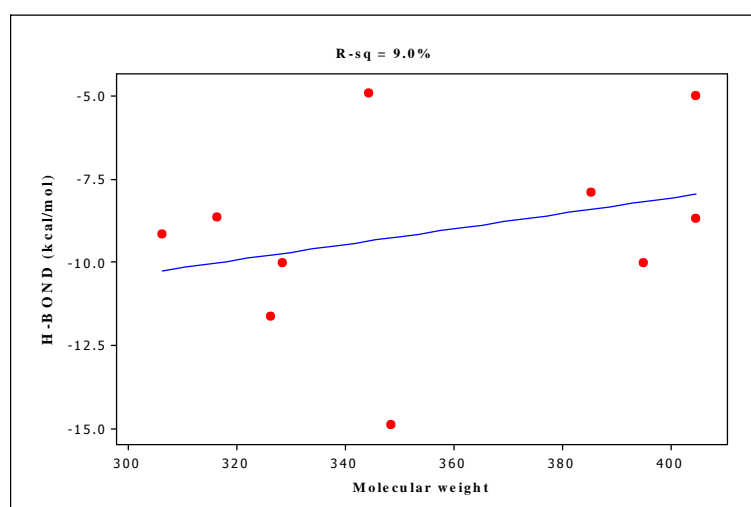
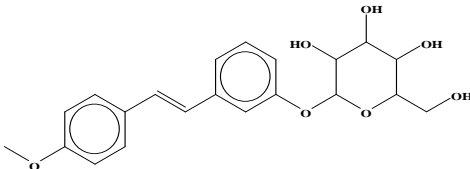
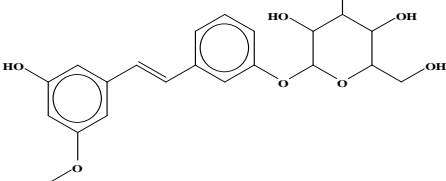
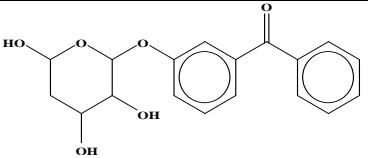
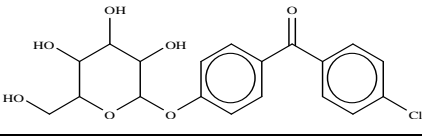
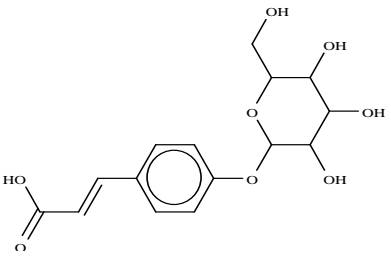
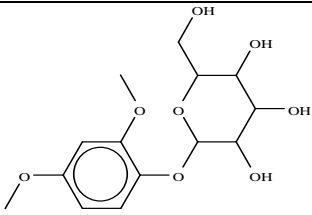
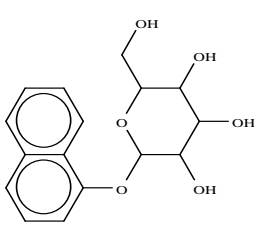


Figure 2. Fitted line plot of the correlation between interaction energy and molecular weight.

In order to have a deep structural insight for the interaction between the selected top ten compounds and our target, further analysis based on both electrostatic and hydrogen bond is carried out (Table 2).

Table 2. Ligand structure, present residues, ligand-protein interaction energy and interaction distances for the top hits.

Compound ID	Structure	Residue	Interaction distance (Å)	Interaction energy (kcal.mol ⁻¹)
Zinc03978768		Met280	3.00	-2.50
		Met280	2.55	-2.12
		His263	2.94	-0.31
		His61	3.35	-1.23
		His85	3.10	-2.50
Zinc31160316		Met280	2.82	-2.50
		Met280	2.86	-2.50
Zinc28002398		Met280	3.12	-2.42
		Met280	2.60	-2.50
Zinc28005633		Met280	3.02	-2.50
		Met280	2.60	-2.50
		His85	2.85	-2.50
		His61	3.10	-2.49
Zinc13542698		Glu322	2.95	-2.50
		His85	3.24	-1.82
		His85	3.47	-0.63
		His61	2.87	-2.50
		Ser282	3.34	-0.43
		Val283	2.96	-1.47
		Met280	2.27	0.25
		Asn260	3.10	-2.50
Zinc38213972		Met280	3.36	-1.19
		Val283	3.11	-2.46
		Asn260	2.93	-2.50
		Gly281	3.10	-2.50
Zinc05665673		Gly86	3.42	-0.92
		Gly86	3.48	-0.61
		Met319	2.64	-2.50
		Arg321	2.58	-2.30
		Arg321	3.28	-1.03
		Ala246	2.84	-2.50
Glu322	2.67	-2.50		
Glu322	3.09	-2.50		

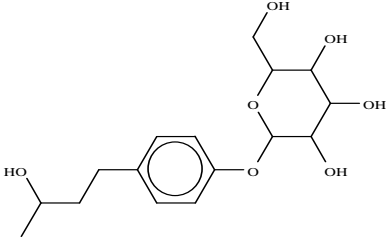
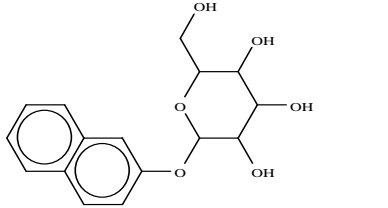
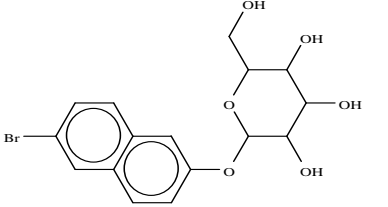
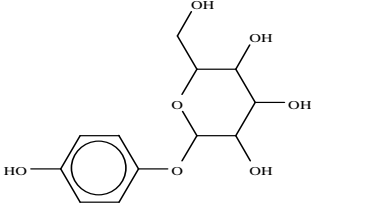
Zinc67902575		Met280	2.90	-2.50
		Met280	2.83	-2.50
		Glu322	2.68	-2.50
		His85	2.69	-2.50
Zinc04201163		Glu256	2.63	-2.50
		Asn260	3.40	-1.02
		Asn260	3.04	-2.50
		Asn260	3.41	-0.96
		His244	3.17	-2.17
Zinc03149174		His85	2.60	-2.50
		His61	3.48	-0.59
		His263	3.25	-1.76
		Met280	2.37	-0.55
		Asn260	3.03	-2.50
Arbutin		Asn260	2.95	-2.50
		Asn260	3.50	-0.25
		Met280	2.61	-2.50
		Met280	2.60	-2.50
		His85	2.96	-2.50
		His244	3.10	-2.50

Table 2 collects the major predicted interactions between the top ten hits and the tyrosinase active site residues, exhibiting the interaction energy ligand-protein, the present residues and the interaction distances. The binding modes of the top hits reveal that the latter were found to be docked into the binding site of tyrosinase (Fig. 3).

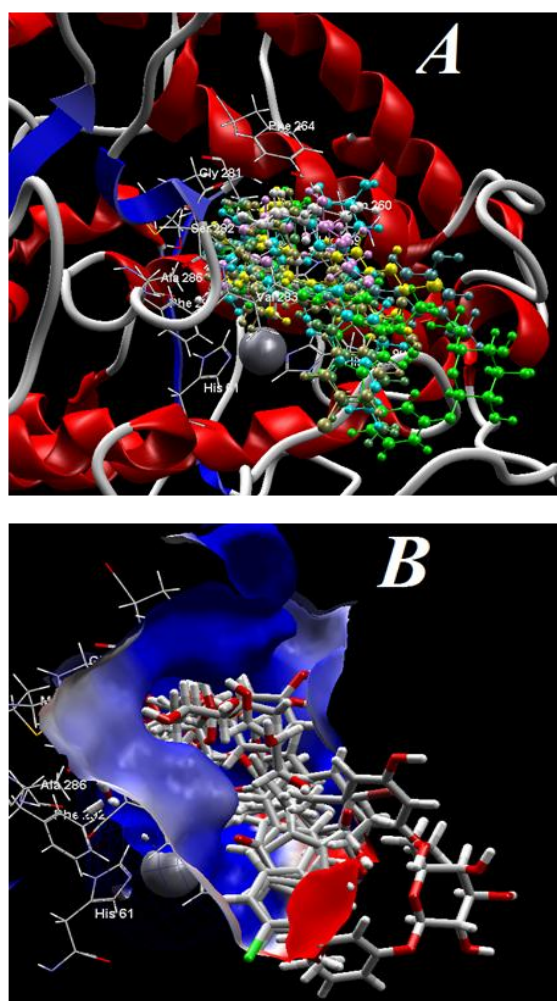


Figure 3. a) Top ten hits docked into the active site of tyrosinase and b) electrostatic surface view of tyrosinase showing the top ten docking hits inside the binding site.

According to the different binding modes of the top ten hits, it is observed that the interactions with the amino acids Met280, His85, His61 and Asn260 of the tyrosinase active site are the most predominant among the top hits. It is also observed that the top four hits Zinc03978768, Zinc28005633, Zinc13542698 and Zinc03149174 have a common interaction with the Met280, His85 and His61 residues of tyrosinase.

The top-scored pose Zinc03978768 forms five hydrogen bonds with four amino acid residues (Fig. 4). The oxygen atom (ID 31) of hydroxyl group mediated a hydrogen bond with Oxygen atom (ID 2280) of Met280 at distance of 2.55Å. The same atom of top-scored pose is also involved in a hydrogen bonding interaction with nitrogen atom (ID 2150) of His263 at distance of 2.94Å. The oxygen atom (ID 32) of hydroxyl group formed a hydrogen bond with the oxygen atom (ID 2280) of Met280 at distance of 3.00Å. Finally, two hydrogen bonds were formed between the oxygen atoms (ID 29 and 30) with nitrogen atoms (ID 484 and ID 684) of His61 and Met85 residues respectively. The positions in the active site of tyrosinase and the binding modes of the top two compounds (Zinc03978768 and Zinc31160316) and arbutin are shown in figure 4, figure 5 and figure 6 respectively. The comparison between binding modes of these compounds reveals that the binding affinity of Zinc03978768 and Zinc31160316 with the active site residues of tyrosinase is more favorable than that of arbutin.

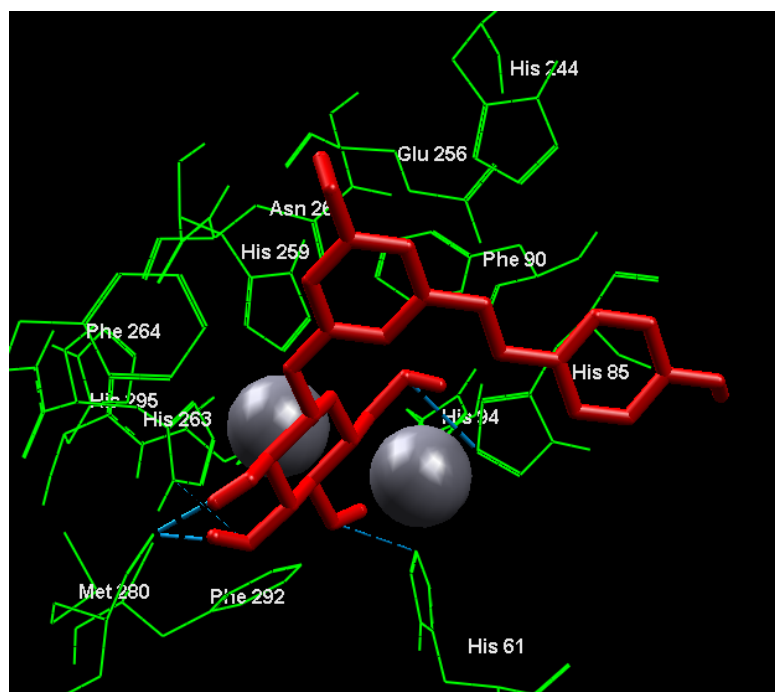


Figure 4. Predicted H-bond interactions (blue dashed lines) between Zinc03978768 (red) and His263, His61, His85, Met280 residues of tyrosinase enzyme.

The rule of five, described by Lipinski et al [27, 28], states that most drug-like molecules have values of LogP (the logarithm of octanol/water partition coefficient) < 5, MW(molecular weight) < 500, HBA(number of hydrogen bond acceptors) < 10 and HBD (number of hydrogen bond donors) < 5. Molecules do not respect these rules may have problem with bioavailability [29].

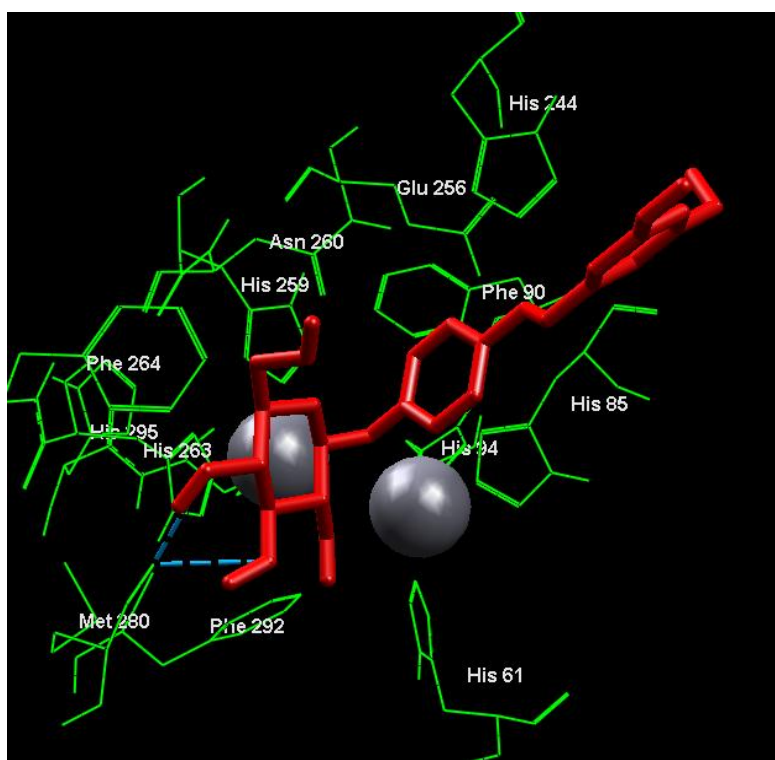


Figure 5. Predicted H-bond interactions (blue dashed lines) linking Zinc31160316 (red) with Met280 residue of tyrosinase enzyme.

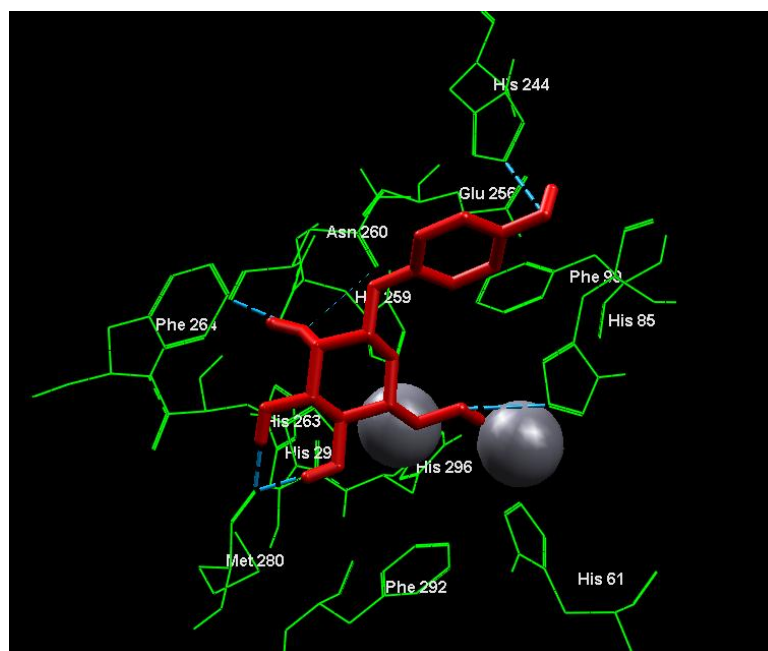


Figure 6. Predicted H-bond interactions (blue dashed lines) between arbutin (red) and Met280, His85, Asn260, His244 residues of tyrosinase enzyme.

Table 3 represents the parameters values of the rule of five for the top ranked hits, arbutin and the experimentally known tyrosinase inhibitors. According to the values showed in table3, all the top ranked hits used in this work abide by the Lipinski rule and may be active compounds.

Table 3. Parameters values of the Lipinski rule for the top hits and arbutin.

Compound ID	LogP ^a	MW ^b	HBA ^c	HBD ^d	TPSA ^e	ROT-B ^f
Zinc03978768	1.74	404.415	8	5	129	6
Zinc31160316	1.74	404.415	8	5	129	6
Zinc28002398	1.98	344.363	6	3	96	4
Zinc28005633	1.80	394.807	7	4	116	5
Zinc13542698	-0.36	325.293	8	4	140	5
Zinc38213972	-0.29	316.306	8	4	118	5
Zinc05665673	1.40	348.351	7	4	108	5
Zinc67902575	0.10	328.361	7	5	120	6
Zinc04201163	0.85	306.314	6	4	99	3
Zinc03149174	1.64	385.21	6	4	99	3
Arbutin	-0.81	272.253	7	5	119	3

^a: The logarithm of octanol/water partition coefficient.

^b: The molecular weight.

^c: The number of hydrogen bond acceptors.

^d: The number of hydrogen bond donors.

^e: The topological polar surface area.

^f: The number of rotatable bonds.

4. CONCLUSION

In this work, molecular docking studies were performed on arbutin analogues retrieved from the Zinc database. The results obtained from docking indicate that some analogues showed a higher Moldock score (in terms of negative energy) compared to arbutin and the experimentally known tyrosinase inhibitors. The top ten ranked hits showed better interaction than arbutin, showing a common molecular interaction with the Met280, His85, His61 and Asn260 residues of the tyrosinase enzyme. Furthermore, these ten docked hits abide by Lipinski's rule of five, stating that these molecules have no problem with bioavailability.

5. ACKNOWLEDGMENTS

This study was supported by "la direction générale de la recherche scientifique et de développement technologique (DGRSDT)" of Algerian Ministry of Scientific Research. The authors would like to dedicate this work to the memory of their colleague Dr.AZZOUZI Abdelkader.

REFERENCES

- [1] Cragg G. & Newman D., 2013. Natural products: a continuing source of novel drug leads, *Biochimica et Biophysica Acta*, Vol. 1830(6), 3670-3695.
- [2] Christaki E., Bonos E., Giannenas I. & Florou-Paneri P., 2012. Aromatic Plants as a Source of Bioactive Compounds, *Agriculture*, Vol. 2, 228-24.
- [3] Shakya S., 2015. Medicinal uses of ginger (*zingiber officinale roscoe*) improves growth and enhances immunity in aquaculture, *International Journal of Chemical Studies*, Vol. 3(2), 83-87.
- [4] Veeresham C., 2012. Natural products derived from plants as a source of drugs, *Journal of Advanced Pharmaceutical Technology & Research*, Vol. 3 (4), 200-201.
- [5] Atanasov A., Waltenberger B., Pferschy-Wenzig E., Linder T., Wawrosch C., Uhrin P., Temml V., Wang L., Schwaiger S., Heiss E. H., Rollinger J. M., Schuster D., Breuss J. M., Bochkov V., Mihovilovic M. D., Kopp B., Bauer R., Dirsch V. M. & Stuppner H., 2015. Discovery and resupply of pharmacologically active plant-derived natural products, *Biotechnology Advances*, Vol. 33(8), 1582-1614.
- [6] Atanasov A. G., Waltenberger B., Pferschy-Wenzig EM., Linder T., Wawrosch C., Uhrin P., Temml V., Wang L., Schwaiger S., Heiss E. H., Rollinger J. M., Schuster D., Breuss J. M., Bochkov V., Mihovilovic M. D., Kopp B., Bauer R., Dirsch V. M. & Stuppner H., 2015. Discovery and resupply of pharmacologically active plant-derived natural products: A review, *Biotechnology Advances*, Vol. 33(8), 1582-1614.
- [7] Sarg T., Abdel- Ghani A., Zayed R. & El-Sayed M., 2012. Bioactive compounds from *Phyllanthus atropurpureus*, *Journal of Natural Products*, Vol. 5, 10-20.
- [8] ElhassanTaha M. M., SalehSalga M., MohdAli H., AmeenAbdulla M., IbrahimAbdelwahab S. & Hadi A., 2012. Gastroprotective activities of *Turnera diffusa Willd. ex Schult. revisited: Role of arbutin*. *Journal of Ethnopharmacology*, Vol. 141 (1), 273-281.
- [9] Kajiwara R., Seto A., Kofujita H., Shiba Y., Oishi Y. & Shibasaki Y., 2019. Enhanced antimicrobial activities of polymerized arbutin and its derivatives prepared by oxidative polymerization of arbutin, *Reactive and Functional Polymers*, Vol. 138, 39-45.
- [10] Migas P. & Krauze-Baranowska M., 2015. The significance of arbutin and its derivatives in therapy and cosmetics, *Phytochemistry Letters*, Vol. 13, 35-40.
- [11] Raudone L., Vilkičkyte G., Pitkauskaitė L., Raudonis R., Vainoriene R. & Motiekaityte V., 2019. Antioxidant Activities of *Vaccinium vitis-idaea L. Leaves within Cultivars and Their Phenolic Compounds*, *Molecules*, Vol. 24 (5), 844-863.
- [12] Ahmadian S. R., Ghasemi-Kasman M., Pouramir M. & Sadeghi F., 2019. Arbutin attenuates cognitive impairment and inflammatory response in pentylenetetrazol-induced kindling model of epilepsy, *Neuropharmacology*, Vol. 146, 117-127.
- [13] Jiang L., Wang D., Zhang Y., Li J., Wu Z., Wang Z. & Wang D., 2018. Investigation of the pro-apoptotic effects of arbutin and its acetylated derivative on murine melanoma cells, *International Journal of Molecular Medicine*, Vol. 4 (2), 1048-1054.
- [14] Garcia-Jimenez A., Teruel-Puche JA., Berna J., Rodriguez-Lopez JN., Tudela J. & Garcia-Canovas F.,

2017. Action of tyrosinase on alpha and beta-arbutin: A kinetic study, *PLoS One*, Vol. 12 (5), 1-19.
- [15] Zhu X., Tian Y., Zhang W., Zhang T., Guang C. & Mu W., 2018. Recent progress on biological production of α -arbutin, *Applied Microbiology and Biotechnology*, Vol. 102 (19), 8145-8152.
- [16] Yu F., Pan Z., Qu B., Yu X., Xu K., Deng Y. & Liang F., 2018. Identification of a tyrosinase gene and its functional analysis in melanin synthesis of *Pteria penguin*, *Gene*, Vol. 656, 1-8.
- [17] Zaidi K. U., Ali S. A. & Ali A. S., 2017. Melanogenic effect of purified mushroom tyrosinase on b16f10 melanocytes: a phase contrast and immunofluorescence microscopic study, *Journal of Microscopy and Ultrastructure*, Vol. 5(2), 82-89.
- [18] molegrovirtualdocking.weebly.com
- [19] www.rcsb.org
- [20] Ismaya W. T., Rozeboom H. J., Weijn A., Mes J. J., Fusetti F., Wichers H. J. & Dijkstra B. W., 2011. Crystal Structure of *Agaricus Bisporus* Mushroom Tyrosinase: Identity of the Tetramer Subunits and Interaction with Tropolone, *Biochemistry*, Vol. 50, 5477-5486.
- [21] Ismayaa W. T., Tandrasasmitaa O. M., Sundaria S., Diana A., Lai X., Rentnoningrum D. S., Dijkstra B.W., Tjandrawinata R. R. & Rachmawati H., 2017. The light subunit of mushroom *Agaricus bisporus* tyrosinase: Its biological characteristics and implications, *International Journal of Biological Macromolecules*, Vol. 102, 308-314.
- [22] zinc15.docking.org
- [23] Thomsen R. & Christensen M., 2006. MolDock: a new technique for high-accuracy molecular docking, *Journal of Medicinal Chemistry*, Vol. 49(11), 3315-3321.
- [24] Singh B. K., Park S. H., Lee H. B., Goo Y. H., Kim H. S., Cho S. H., Lee J. H., Ahn G. W., Kim J. P., Kang S. M. & Kim E. K., 2016. Kojic Acid Peptide: A New Compound with Anti-Tyrosinase Potential, *Annals of Dermatology*, Vol. 28(5), 555-561.
- [25] Pillaiyar T., Manickam M. & Namasivayam V., 2017. Skin whitening agents: medicinal chemistry perspective of tyrosinase inhibitors, *Journal of Enzyme Inhibition and Medicinal Chemistry*, Vol. 32(1), 403-425.
- [26] Nairn R., Cresswell W. & Nairn J., 2015. Mushroom Tyrosinase: A Model System to Combine Experimental Investigation of Enzyme-Catalyzed Reactions, Data Handling Using R, and Enzyme-Inhibitor Structural Studies, *Biochemistry and Molecular Biology Education*, Vol. 43(5), 370-376.
- [27] Lipinski C. A., 2000. Drug-like properties and the causes of poor solubility and poor permeability, *Journal of Pharmacological and Toxicological Methods*, Vol. 44, 235-249.
- [28] Lipinski C. A., Lombardo F., Dominy B. W. & Feeney P. J., 1997. Experimental and computational approaches to estimate solubility and permeability in drug discovery and development settings, *Advanced Drug Delivery Reviews*, Vol. 23, 3-25.
- [29] Freitas M.P., 2006. MIA-QSAR modelling of anti-HIV-1 activities of some 2-amino-6-rylsulfonyl benzonitriles and their thio and sulfinyl congeners, *Organic & Biomolecular Chemistry*, Vol. 4, 1154-1159.